Zero-position Offset Calibration of PMSM Based on I/f Control Strategy and Slide Mode Observer for Electric Power Steering System

Yingzhe Wu[1*], Hui Li[2*], Lisheng Wang[1], Shan Yin[2]
[1] Beijing Research & Development Center, Shanghai Gatek Automotive Electronics Co.,Ltd, Beijing, China
[2] School of Aeronautics & Astronautics, University of Electronic Science and Technology of China, Chengdu, China
Email: microuestc@163.com[1*]; kelly.li@126.com[2*]

***Abstract*—In this paper, I/f control strategy combined with slide mode observer (SMO) are applied to calibrate the zero-position offset between permanent magnet synchronous motor (PMSM) and its rotor position sensor (RPS) for electric power steering (EPS) system. The I/f control strategy can ensure the motor operates in a medium speed smoothly with full torque capacity; while the SMO offers a reliable estimation of the rotor position of the motor itself. As a result, the offset between motor and its RPS can be acquired. In addition, the time delay caused by process time and sampling period of the digital controller has also been analyzed. According to experiment result, it can be figured out that the proposed method can accurately align the zero-position offset angle whether the motor operates on-load or off-load, which is critical for EPS production line.**

***Index Terms*—Zero-position offset calibration, permanent magnet synchronous motor (PMSM), rotor position sensor (RPS), electric power steering (EPS).**

I. Introduction

The permanent magnet synchronous motor (PMSM) has become one of the most popular choices for electric power steering (EPS) system due to its superiorities in vibration, noise, and efficiency [1]–[5]. The PMSM is usually considered as an actuator of EPS system, which regulates the torque on the steering column, following some predefined torque-angle characteristic curve [4], [6], [7]. Therefore, the field oriented control (FOC) algorithm can be adopted to regulate the torque of the PMSM by controlling the d-q axis current directly [8]–[10]. It is noted that the rotor position of the motor is one of the most important factors in realization of FOC. A reliable information of the rotor position can ensure the motor operating in maximum torque per ampere (MTPA) region within the rated speed [11]. As a result, the high-precision rotor position sensors (RPS), such as Magneto-Resistive (MR) sensor and resolver, have been widely used to acquire more accurate rotor position [4], [12], [13]. However, there is an inevitable zero-position offset angle ($\Delta\theta$ illustrated in Fig. 1) existing between PMSM and its RPS.

$$\Delta\theta = \theta_{RPS} - \theta_{Rotor} \tag{1}$$

Where, θ_{Rotor} is the rotor position of the PMSM and θ_{RPS} represents the output angle of the RPS. In [9], the authors claim that an apparent torque decrease will be caused once the offset angle exceeds 12°. In some applications, such offset can be maintained in a reasonable range with assistance of a specialized fixture. But it also requires further calibration to maintain an acceptable control performance. Obviously, it is a feasible way to compensate the offset effectively based on well designed algorithm instead of special developed fixture and reduce the cost in industry applications.

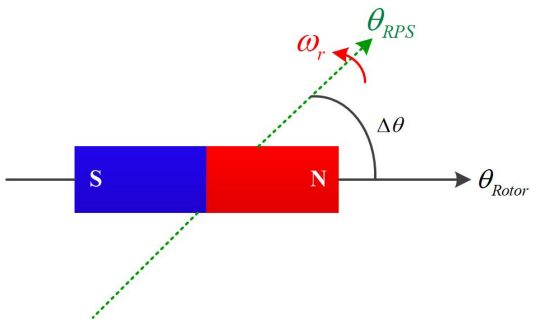

Fig. 1. Zero-position offset between PMSM and its RPS.

In recent years, several calibration methods were proposed to align the position sensor offset between PMSM and its RPS [10], [11], [14]–[16]. Although the methods can effectively compensate the offset, they are still not suitable for applying in EPS production line due to several reasons (will be explained in Section II). Fig. 2 shows two types of EPS control unit at the end of line (EOL). The type I is considered as a control unit integrated with the motor and electronic control unit (ECU), and the motor in this case is off-load; while the type II is considered as a sub-system integrated with motor, ECU, and steering column together, and the motor in this situation is viewed as on-load. It is obvious that the calibration method for EPS production line should be effective whether the motor is on-load or off-load.

In this paper, a calibration method combined with I/f control strategy and slide mode observer (SMO) is proposed to align the zero-position offset between PMSM and its RPS for EPS production line. For one thing, the I/f control strategy can ensure the motor operates in a medium speed smoothly with full load capacity; for another, the SMO offers a reliable estimation of the rotor position of the motor itself. As a result, the offset between motor and RPS can be aligned whenever the motor is on-load or off-load.

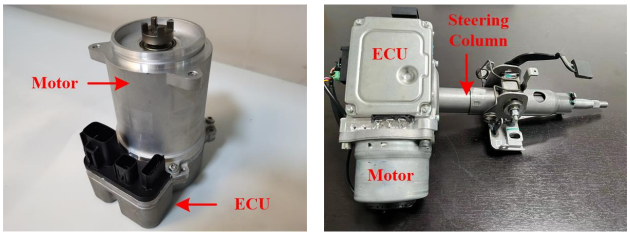

(a) (b)

Fig. 2. Two types of EPS control unit at the end of line (EOL), (a) Type I: integrated motor and ECU, (b) Type II: integrated motor, ECU, and steering column.

The rest of this paper is organized as follows. Section II gives a brief review of the existing calibration methods. The calibration method combined with I/f control strategy and SMO is elaborated in Section III, and experiment verification is carried out in Section IV. Finally, the conclusion and future works are summarized in Section V.

II. Review of Existing Position Sensor Offset Calibration Methods of PMSM

Method 1: A simple method for zero-position offset alignment is realized based on six fundamental space voltage vectors shown in Fig. 3 [11]. The ECU can generate the fundamental voltage vectors periodically and lock the rotor located at a certain position, which is demonstrated in Table.I. Then, the zero-position offset can be easily acquired based on the relationship described in Table. I. However, this method is only suitable for off-load calibration. Once the motor operates on-load, variations in align current, initial position, and load torque will impact steady-state value of the calibrated offset angle significantly, which causes unreliable result [11]. In addition, the method will also cause a large current surge during starting-stage of the motor, which largely increases current stress of the inverter.

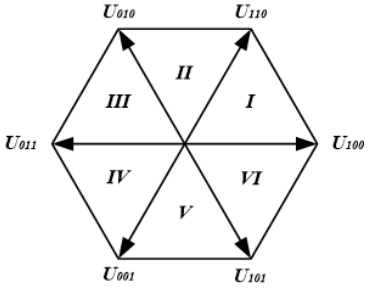

Fig. 3. Fundamental space voltage vectors in motor drives.

Method 2: High-frequency (HF) signal injection method was also well demonstrated in [11]. Fig. 4 illustrates relationships between virtual (d'-q') and real (d-q) synchronous rotation references of the motor. Assuming that:

$$\begin{cases} u_d' = u_{in} \cdot \cos\left(\omega_{in} \cdot t\right) \\ u_q' = 0 \end{cases} \tag{2}$$

TABLE I. Relationship between space voltage vector and electrical-angle of the motor

Sector Number	I	II	III	IV	V	VI
Vectors	U_{100}	U_{110}	U_{010}	U_{011}	U_{001}	U_{101}
Angle	0°	60°	120°	180°	240°	300°

in which, u_d' and u_q' represent the voltage applied on the virtual synchronous rotation reference, u_{in} and ω_{in} can be considered as the amplitude and frequency of the injected HF signal. Then, the following expressions can be acquired according to the principle elaborated in [11], [17].

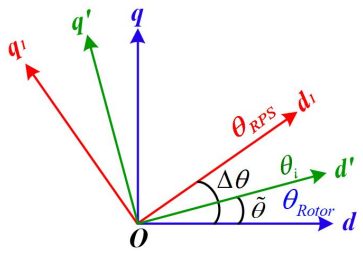

Fig. 4. Relationships between virtual (d'-q') and real (d-q) synchronous rotation references.

$$i_d{}' = \frac{u_{in}\sin\left(\omega_{in}t\right)}{L^2 - \Delta L^2} \cdot \left[L + \cos\left(2\tilde{\theta}\right)\Delta L\right] \tag{3}$$

$$i_q{}' = \frac{u_{in}\sin\left(\omega_{in}t\right)}{L^2 - \Delta L^2} \cdot \sin\left(2\tilde{\theta}\right)\Delta L \tag{4}$$

Where, i_d' and i_q' are the measured current on the virtual synchronous rotation reference, L=(L_d+L_q)/2, ΔL=(L_q-L_d)/2, and $\tilde{\theta}$ =θ_{Rotor}-θ_i. The simulation result of the HF injection method is given in Fig. 5. The zero-crossing point of i_q' means that θ_{Rotor}=$k\pi$/2+θ_i, where k=0, ±1, ±2, and ±3. Thus, the offset angle can be obtained as $\Delta\theta$=θ_{RPS}-($k\pi$/2+θ_i). It is noted that the HF injection method can effectively compensate the offset for the motor with higher salient rate ($\rho \geq 1.5$). However, it shows a reduced accuracy for the surface-mounted PMSM or the motor with lower salient rate. In addition, extraction of $\tilde{\theta}$ based on Equ. (4) is rather complicated because it contains various digital filter design.

Method 3: Calibration method based on dynamo test setup has been proposed in [10], [14], [15]. During calibration process, the dynamo test setup offers a constant rotation speed in a medium range. Then, according to the principles elaborated in [10], [14], [15], the zero-position offset between motor and RPS can be acquired effectively. However, the external dynamo test setup increases the complexity and the cost of the EPS production line. In order to remove the dynamo system in calibration, an off-load method is proposed and verified in [16]. However, it seems less effective when the motor is on-load, such as the situation II illustrated in Fig. 2 (b).

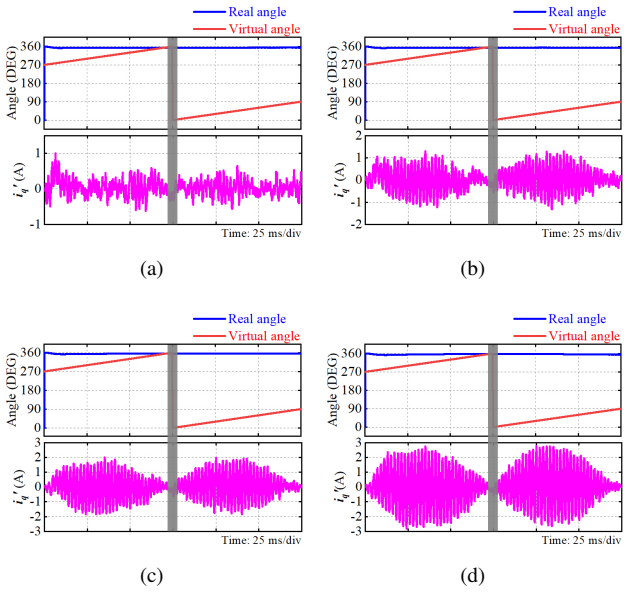

Fig. 5. Simulated waveforms of i_q' based on HF signal injection method , (a) L_q=L_d, (b) L_q=1.25L_d, (c) L_q=1.5L_d, (d) L_q=2L_d.

III. Calibration Method Based on I/f Control Strategy and Slide Mode Observer

A. I/f Control Strategy of PMSM

I/f control can be considered as a speed open-loop and current closed-loop strategy [18], [19], and is suitable for starting the PMSM with full torque capacity in a medium speed smoothly without causing a large current surge. Fig. 6 shows the scheme of the I/f control strategy of the PMSM. Compared with FOC, the rotor position angle of the motor is replaced by synchronous rotating angle (θ_i), which is determined by integration of the reference frequency ($p{\cdot}\omega_i$). Fig. 7 illustrates the relationship between the rotor reference (d-q) and the synchronous rotating reference (d'-q') of the PMSM with I/f control strategy. Thus, the generated torque

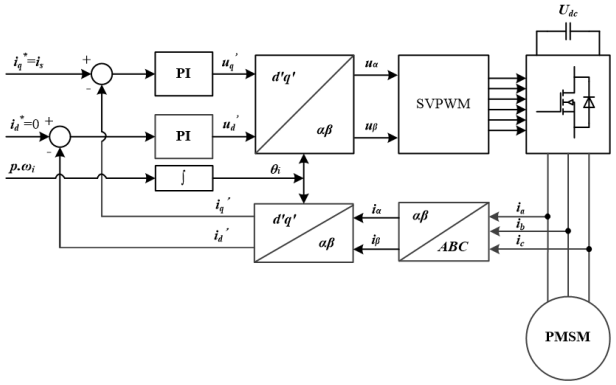

Fig. 6. Scheme of the I/f control strategy of PMSM.

of the PMSM (L_d=L_q=L) can be obtained as:

$$T_e = 1.5p\varphi_m i_s \cdot \sin(\delta) \tag{5}$$

where, φ_m is the permanent magnet flux-linkage, i_s is the current of q' axis, p is pole pairs of the motor, and δ is the load angle. By analyzing Fig. 7 and Equ. (5), the characteristic

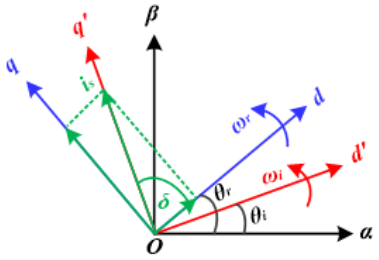

Fig. 7. Rotor reference (d-q) frame and synchronous rotating reference (d'-q') frame of the PMSM.

of the I/f control strategy can be acquired (see Fig. 8). It should be noted that the δ should be always kept in the ranges of $0°{\le}\delta{<}\ 90°$ when $\omega_i{\ge}0$ and $-90°{<}\delta{\le}0°$ when $\omega_i{<}0$ for stable operation [19].

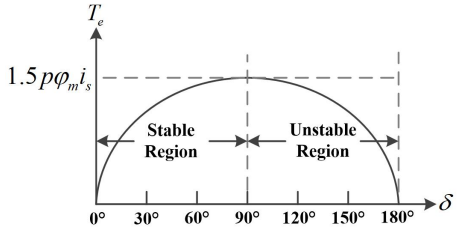

Fig. 8. Characteristic of the I/f control strategy when $\omega_i{\ge}0$.

In this case, p = 4, φ_m = 0.00655 Wb. The load torque (T_L) of the motor is considered as 0.5 N.m, and the torque ripple is no more than 10%. Since T_e usually approximates to $1.5T_L$ during start acceleration stage of the motor, δ varies between 39.5° and 72.7° when i_s is set as 20 A in the whole control process, which can ensure the PMSM operating stably in the I/f control mode with sufficient margin.

B. SMO for Rotor Position Estimation

With the merits of simple structure, strong robustness, and good dynamic performance, SMO is widely used for back-EMF estimation of the PMSM with medium and high rotation speed. According to the principles elaborated in [20], [21], the estimated current and back-EMF in α-β reference of the motor (L_d=L_q=L) can be acquired as:

$$\begin{bmatrix} \hat{i}_\alpha(k+1) \\ \hat{i}_\beta(k+1) \end{bmatrix} = \begin{bmatrix} -\frac{R_s{\cdot}T_s}{L} & 0 \\ 0 & -\frac{R_s{\cdot}T_s}{L} \end{bmatrix} \begin{bmatrix} \hat{i}_\alpha(k) \\ \hat{i}_\beta(k) \end{bmatrix} + \begin{bmatrix} \hat{i}_\alpha(k) \\ \hat{i}_\beta(k) \end{bmatrix} + \frac{T_s}{L} \begin{bmatrix} u_\alpha(k) \\ u_\beta(k) \end{bmatrix} - \frac{T_s}{L} \begin{bmatrix} h \cdot sign\left(\hat{i}_\alpha(k) - i_\alpha(k)\right) \\ h \cdot sign\left(\hat{i}_\beta(k) - i_\beta(k)\right) \end{bmatrix} \tag{6}$$

$$\begin{bmatrix} \hat{E}_\alpha(k+1) \\ \hat{E}_\beta(k+1) \end{bmatrix} = -\frac{L}{T_s} \begin{bmatrix} i_\alpha(k+1) \\ i_\beta(k+1) \end{bmatrix} + \begin{bmatrix} -R_s & 0 \\ 0 & -R_s \end{bmatrix} \begin{bmatrix} i_\alpha(k) \\ i_\beta(k) \end{bmatrix} + \frac{L}{T_s} \begin{bmatrix} i_\alpha(k) \\ i_\beta(k) \end{bmatrix} + \begin{bmatrix} u_\alpha(k) \\ u_\beta(k) \end{bmatrix} \tag{7}$$

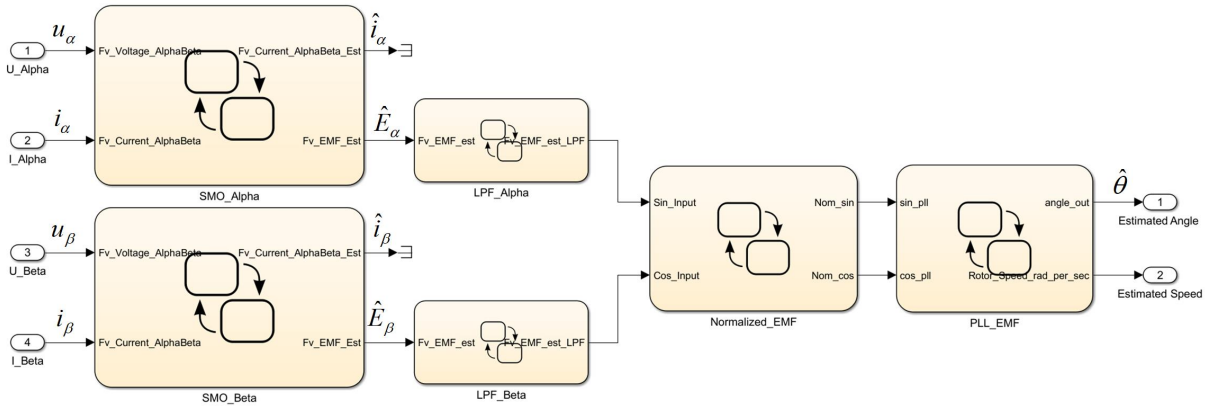

Fig. 9. Scheme of SMO for rotor position estimation of PMSM.

where, i_α and i_β are actual current in α-β reference, u_α and u_β are actual voltage in α-β reference, $\hat{i}_\alpha$ and $\hat{i}_\beta$ are estimated current in α-β reference, $\hat{E}_\alpha$ and $\hat{E}_\beta$ are estimated back-EMF in α-β reference, h is slide mode gain, R_s and T_s represent resistance of the motor and sampling period of the digital controller. The $(k+1)$ and (k) indicate the obtained values in the current and the last sampling period.

The scheme of the SMO is shown in Fig. 9. It is noted that the estimated back-EMF contains substantial chattering and harmonics due to the discontinuous characteristic of the SMO. As a result, a low pass filter (LPF) is required. In addition, normalization of the back-EMF is also required to improve the accuracy of the extracted rotor position based on phase lock loop (PLL). On the other hand, the phase delay of the extracted rotor position caused by LPF should also be properly compensated.

C. Time Delay Compensation

In order to acquire reliable offset angle, the time delay caused by process time and sampling period of the digital controller should also be considered. Usually, the motor operates in a medium speed (75 rad/s in this case) can eliminate influence of the dead-time zone of the inverter during calibration. However, the impacts of the time delay become obvious with the increased rotation speed. Fig. 10 illustrates the zero-position offset angle with the influence of the time delay. In this condition, the phase delay angle (α) can be expressed as:

$$\alpha = \omega_r \cdot p \cdot T_s \tag{8}$$

Thus, the following relationships can be obtained as:

$$\begin{cases} \theta^+_{RPS} = \Delta\theta - \alpha & \omega_r \geq 0 \\ \theta^-_{RPS} = \Delta\theta + \alpha & \omega_r < 0 \end{cases} \tag{9}$$

in which, θ^+_{RPS} and θ^-_{RPS} represent the output angle obtained from the RPS with the ECU when $\omega_r \geq 0$ and $\omega_r < 0$, respectively. As a result, the zero-position offset between the PMSM and its RPS can be acquired as:

$$\Delta\theta = \frac{\theta^+_{RPS} + \theta^-_{RPS}}{2} \tag{10}$$

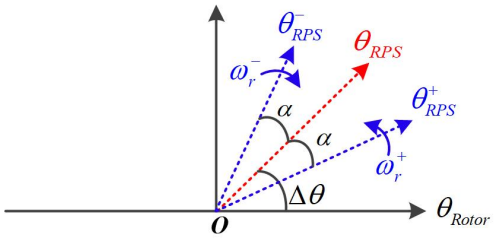

Fig. 10. Zero-position offset between PMSM and its RPS with consideration of time delay caused by sampling period of the digital controller.

IV. Experiment Verification

The test bench of the proposed position sensor offset calibration method is given in Fig. 11. It is noted that the on-load test is implemented with the motor fixed on the steering column, and the off-load test is carried out by connecting the motor with ECU through copper wires. A 12-V battery offers the power supply for the whole control unit. The ECU is communicated with the host computer through CAN bus. Additionally, ω_r and i_s are set as $\pm$75 rad/s and 20 A, respectively.

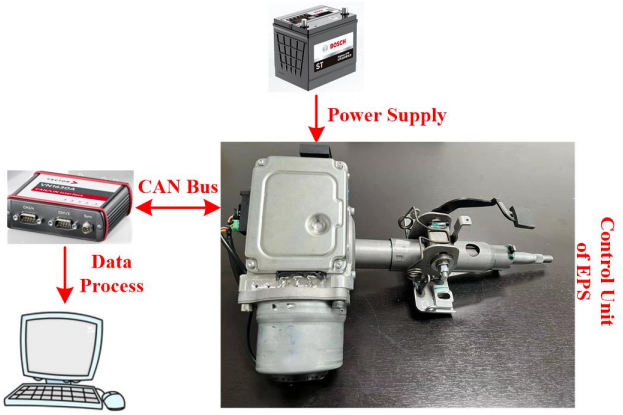

Fig. 11. Test bench of position sensor offset calibration for EPS.

Figs. 12 and 13 present the test results of the motor operates in off-load and on-load conditions (ω_r = +75 rad/s and i_s = 20 A). It can be found that the estimated normalized back-EMF is rather stable, and the observed α-β axis current based on SMO is also in good agreement with the measured one, which indicates that the estimated rotor position is in sufficient accuracy.

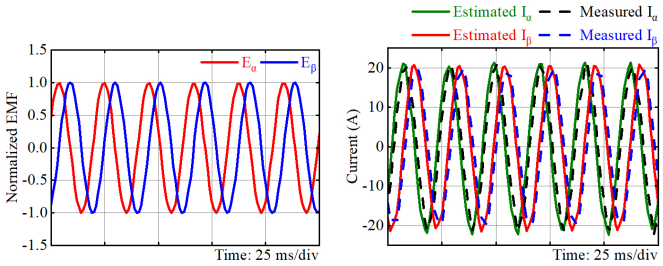

(a) (b)

Fig. 12. Test results of the motor operates in off-load condition (ω_r = +75 rad/s and i_s = 20 A), (a) Estimated back-EMF in normalized value, (b) Measured and estimated α-β axis current.

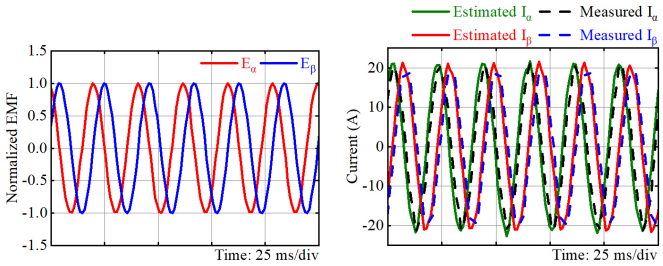

(a) (b)

Fig. 13. Test results of the motor operates in on-load condition (ω_r = +75 rad/s and i_s = 20 A), (a) Estimated back-EMF in normalized value, (b) Measured and estimated α-β axis current.

Figs. 14 and 15 give the measured and estimated rotor position when the motor operates in off-load and on-load conditions. Then, the position sensor offset angle can be acquired accordingly (see Fig. 16). As ω_r = 75 rad/s, p = 4, and T_s = 150 μs in this case, the phase delay angle (α) can be calculated as 2.58° based on Equ. (8). However, it is not in accordance with the results shown in Table II, which may be attributed to the steady-state error caused by SMO and deserves special attention in the future study.

TABLE II. Mean value of offset angle and phase delay angle

Motor Condition	$\Delta\theta^+_{RPS}$	$\Delta\theta^-_{RPS}$	α
Off-load	137.01°	130.01°	-3.5°
On-load	135.52°	131.55°	-2.0°

With the time delay compensation demonstrated in Equ. (10), the zero-position offset between the PMSM and its

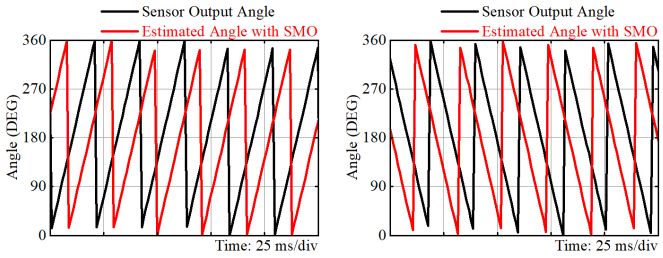

(a) (b)

Fig. 14. Measured and estimated rotor position when motor operates in off-load condition (ω_r = ±75 rad/s and i_s = 20 A), (a) ω_r = +75 rad/s, (b) ω_r = -75 rad/s.

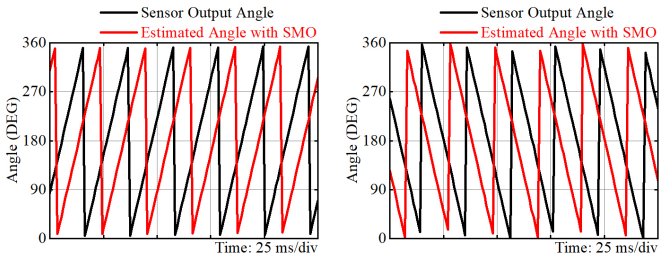

(a) (b)

Fig. 15. Measured and estimated rotor position when motor operates in on-load condition (ω_r = ±75 rad/s and i_s = 20 A), (a) ω_r = +75 rad/s, (b) ω_r = -75 rad/s.

RPS can be obtained (see Fig. 17). The mean value of the zero-position offset calibrated with different methods is also summarized in Table. III. Although there are some deviations existing between different calibration methods (the maximum deviation value is around 4.1°), it can also be considered that the proposed method is able to effectively calibrate the offset angle in both on-load and off-load conditions. In addition, it is interesting to observed that the deviation between on-load and off-load calibration is only 0.03° with the proposed method, which further verifies its effectiveness.

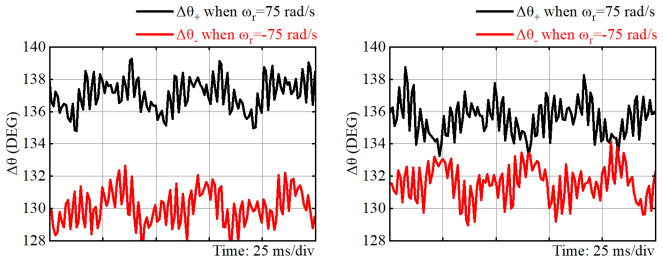

(a) (b)

Fig. 16. Position sensor offset angle when motor operates in off-load and on-load conditions (ω_r = ±75 rad/s and i_s = 20 A), (a) Off-load, (b) On-load.

TABLE III. Mean value of the offset angle calibrated with different methods

Calibration Method	Method 1 [11]	Method 3 [10]	Proposed in this paper	Proposed in this paper
Motor Condition	Off-Load	Speed Load (80 rad/s)	Off-Load	Torque Load (0.5 N.m)
$\Delta\theta$ **(Mean Value)**	$136.80°$	$137.64°$	$133.51°$	$133.54°$

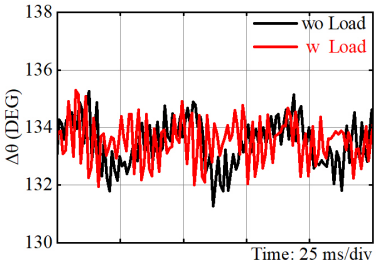

Fig. 17. Zero-position offset angle between PMSM and its RPS.

V. Conclusion and Future Works

In this paper, I/f control strategy combined with SMO are applied to calibrate zero-position offset between PMSM and its RPS for EPS system. The experiment results indicate that there is a slight deviation ($0.03°$) existing between the aligned offset angle when motor is on-load and off-load with the proposed method. The maximum deviation is about $4.1°$ compared with the other calibration methods, which may be attributed to the steady-state error cause by SMO. Although such deviation existing, it can also be considered that the proposed method is able to effectively calibrate zero-position offset angle whether the motor is on-load or off-load. Moreover, the method is easily carried out without any extra test equipment, such as specialized fixture and dynamo test setup. Thus, it is suitable for applying in EPS production line. In the future study, an improved SMO should be considered to further enhance the accuracy and reliability of the calibration method.

References

[1] K.-Y. Cho, Y.-K. Lee, H. Mok, H.-W. Kim, B.-H. Jun, and Y. Cho, "Torque ripple reduction of a PM synchronous motor for electric power steering using a low resolution position sensor," *J. Power Electron.*, vol. 10, no. 6, pp. 709–716, 2010.

[2] A.-M. Nicorici, M. Ruba, C. S. Martis, L. Szabo, and Z. Mathe, "Comparative analysis of permanent magnet synchronous machines designed for electric power steering applications," in *Proc. International Conference on Electrical Power Drive Systems (ICEPDS)*, St. Petersburg, Oct. 2020, pp. 1–6.

[3] H. Akhondi, J. Milimonfared, and K. Malekian, "Performance evaluation of electric power steering with ipm motor and drive system," in *Proc. International Power Electronics and Motion Control Conference*, Poznan, Sep. 2008, pp. 2071–2075.

[4] G. Lee, W. Choi, S. Kim, S. Kwon, and J. Hong, "Torque ripple minimization control of permanent magnet synchronous motors for EPS applications," *Int. J. Automot. Technol.*, vol. 12, no. 2, pp. 291–297, 2011.

[5] R. R. Sorial, M. H. Soliman, H. M. Hasanien, and H. E. A. Talaat, "A vector controlled drive system for electrically power assisted steering using hall-effect sensors," *IEEE Access*, vol. 9, pp. 116 485–116 499, 2021.

[6] D. Lee, K.-S. Kim, and S. Kim, "Controller design of an electric power steering system," *IEEE Trans. Control Syst. Technol.*, vol. 26, no. 2, pp. 748–755, 2018.

[7] A. Zaremba, M. Liubakka, and R. Stuntz, "Control and steering feel issues in the design of an electric power steering system," in *Proc. American Control Conference (ACC)*, vol. 1, Philadelphia, Jun. 1998, pp. 36–40.

[8] O. C. Kivanc and S. B. Ozturk, "MATLAB function based approach to FOC of PMSM drive," in *Proc. IEEE European Modelling Symposium (EMS)*, Madrid, Oct. 2015, pp. 96–102.

[9] S. S. Kuruppu and Y. Zou, "Post production PMSM position sensor offset error quantification via voltage estimation," in *Proc. IEEE Energy Conversion Congress and Exposition (ECCE)*, Detroit, Oct. 2020, pp. 3355–3361.

[10] S. S. Kuruppu, "In-system calibration of position sensor offset in PMSM drives," in *Proc. IEEE International Electric Machines and Drives Conference (IEMDC)*, Hartford, May 2021, pp. 1–5.

[11] S. Zossak, M. Stulraiter, P. Makys, and M. Sumega, "Initial position detection of PMSM," in *Proc. IEEE International Symposium on Sensorless Control for Electrical Drives (SLED)*, Helsinki, Sep. 2018, pp. 12–17.

[12] R. Bojoi, M. Pastorelli, J. Bottomley, P. Giangrande, and C. Gerada, "Sensorless control of PM motor drives - A technology status review," in *Proc. IEEE Workshop on Electrical Machines Design, Control and Diagnosis (WEMDCD)*, Paris, Mar. 2013, pp. 168–182.

[13] "Kmz60 angle sensor with integrated amplifier," [Online Available]: http://www.nxp.com, accessed: Feb. 2014.

[14] J.-Y. Park, Y.-K. Ko, D.-Y. Jang, M.-S. Kwak, and Y.-K. Lee, "Auto calibration of position sensor while driving ECO vehicle," in *Proc. IEEE Transportation Electrification Conference and Expo, Asia-Pacific (ITEC Asia-Pacific)*, Busan, Jun. 2016, pp. 397–401.

[15] J. S. Bang and T. S. Kim, "Automatic calibration of a resolver offset of permanent magnet synchronous motors for hybrid electric vehicles," in *Proc. American Control Conference (ACC)*, Chicago, Jul. 2015, pp. 4174–4179.

[16] D. Kim, J. Kim, H. Lim, J. Park, J. Han, and G. Lee, "A sudy on accurate initial rotor position offset detection for a permanent magnet synchronous motor under a no-Load condition," *IEEE Access*, vol. 9, pp. 73 662–73 670, 2021.

[17] R. Filka, P. Balazovic, and B. Dobrucky, "Transducerless speed control with initial position detection for low cost PMSM drives," in *Proc. International Power Electronics and Motion Control Conference*, Poznan, Sep. 2008, pp. 1402–1408.

[18] M. Fatu, R. Teodorescu, I. Boldea, G.-D. Andreescu, and F. Blaabjerg, "I-F starting method with smooth transition to EMF based motion-sensorless vector control of PM synchronous motor/generator," in *Proc. IEEE Power Electronics Specialists Conference*, Rhodes, Jun. 2008, pp. 1481–1487.

[19] S. V. Nair, K. Hatua, N. Durga Prasad, and D. K. Reddy, "Quick and seamless transition method for I-f to sensorless vector control changeover and on-the-fly start of PMSM drives," *IET Electric Power Appl.*, vol. 14, no. 11, pp. 2231–2242, 2020.

[20] Y. Chen, M. Li, Y. Gao, and Z. Chen, "A sliding mode speed and position observer for a surface-mounted PMSM," *ISA Transactions*, vol. 87, pp. 17–27, 2019.

[21] Z. Qiao, T. Shi, Y. Wang, Y. Yan, C. Xia, and X. He, "New sliding-mode observer for position sensorless control of permanent-magnet synchronous motor," *IEEE Trans. Ind. Electron.*, vol. 60, no. 2, pp. 710–719, 2013.